PAPER

Microwave-absorbing properties of room-temperature ionic liquids

IOP Publishing Journal of Physics D: Applied Physics
J. Phys. D: Appl. Phys. **52** (2019) 155302 (10pp) https://doi.org/10.1088/1361-6463/ab016c

Microwave-absorbing properties of room-temperature ionic liquids

Fulong Yang[1,2,3,4], Jianhao Gong[1], E Yang[1], Yongji Guan[1], Xiaodong He[1], Shimin Liu[5], Xiaoping Zhang[1] and Youquan Deng[5]

[1] School of Information Science and Engineering, Lanzhou University, Lanzhou 730000, People's Republic of China
[2] College of Electrical and Information Engineering, Lanzhou University of Technology, Lanzhou 730000, People's Republic of China
[3] Key Laboratory of Gansu Advanced Control for Industrial Processes, Lanzhou University of Technology, Lanzhou 730000, People's Republic of China
[4] National Experimental Teaching Center of Electrical and Control Engineering, Lanzhou University of Technology, Lanzhou 730000, People's Republic of China
[5] Centre for Green Chemistry and Catalysis, Lanzhou Institute of Chemical Physics, CAS, Lanzhou 730000, People's Republic of China

E-mail: zxp@lzu.edu.cn and ydeng@licp.cas.cn

Received 28 October 2018, revised 20 January 2019
Accepted for publication 23 January 2019
Published 11 February 2019

Abstract

Here, the microwave-absorbing properties of 1-ethyl-3-methylimidazolium and 1-butyl-3-methylimidazolium ([E and BMIm]$^+$-based) room-temperature ionic liquids (ILs) with different anions were systematically investigated by measuring dielectric properties in the 1–14 GHz microwave-frequency range. First, the dielectric properties of the [E and BMIm]$^+$-based ILs were studied with a typical open-ended coaxial probe system. The results showed that the real part of permittivity ε' values decreased from 13 to 4 and the values of loss tangent decreased from 5.91 to 0.24, meaning that ILs displayed high dielectric-loss characteristics at microwave-frequency ranges. Furthermore, it was found that the conductivity loss was dominant for dielectric loss in the low-frequency band, and the polarization loss played a major role in high-frequency bands. For the same anion ILs with different cations, the permittivity became higher as the length of the alkyl chain decreased. The absorption properties of [E and BMIm]$^+$-based ILs could be obtained based on their dielectric properties, and found the ILs absorption bands were mainly concentrated in the C band and X band. It was noted that the maximum reflection loss (RL) of [BMIm][NTf_2] with a thickness of 4 mm reached −27.6 dB at 8.73 GHz, and the bandwidth of an RL less than −10 dB could be up to 4.3 GHz. The absorption peak frequency of the ILs gradually shifted to lower frequencies with increasing temperature and coating thickness, which might be caused by the change in impedance matching.

Keywords: ionic liquids, microwave-absorbing, dielectric properties

(Some figures may appear in colour only in the online journal)

1. Introduction

Microwave-absorbing materials have received much attention because of their prospective applications in electronic instruments, industry, commerce, and military affairs [1]. Most of the microwave-absorbing materials are in the solid state, composed of magnetic-loss powders such as ferrite [2], nickel [3], and cobalt [4], and dielectric-loss materials such as composite ceramics [5, 6], carbon nanotubes (CNTs) [7], conducting polymers [8], and graphene [9, 10]. However, liquid-state-absorbing materials are rarely the object of concern due to their absorption efficiency. Recently, liquid water has been considered as

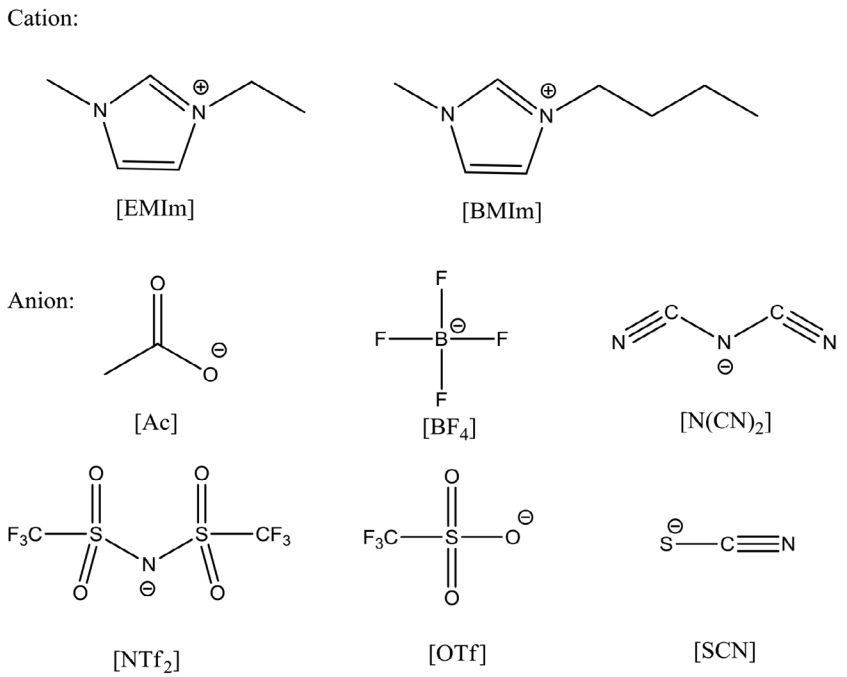

Figure 1. Structures of methylimidazolium ILs with different anions and cations.

a material platform for a new structural microwave-absorbing material [11, 12] that can achieve perfect absorption in the Ku, K, and Ka bands. It is possible to control the absorption ratio and absorption wavelength band of electromagnetic waves according to the shape of water droplets, as well as their height and diameter. Compared with solid-state microwave-absorbing material, structural-absorbing material with liquid water has the advantages of reconstruction, easy tunability, low cost, wide-frequency band, and small density. However, it has the disadvantages of volatility, poor thermal stability, and easy vaporization or condensation. It is therefore urgent to find new kinds of liquid materials to overcome the weaknesses of water.

Room-temperature ionic liquids (RTILs) are a novel class of versatile solvents and soft materials possessing unique physico-chemical properties, including negligible vapor pressure, wide liquid range, intrinsic ionic conductivity, acceptable electrochemical stability, and environmental friendliness [13–15]. Apart from these well-known properties, the most important characteristic of ILs is that their properties can be significantly regulated for any particular application by changing their combination of ions. This makes them 'designable materials'. Their dielectric properties are considered to present unique opportunities to study the microwave-absorbing properties and the fundamental dynamics of RTILs. Early reports were initially focused on extrapolating the 'static dielectric constants' from frequency-dependent measurements [16–18], but much progress had been made within the last several decades in also extracting dynamical information from broadband dielectric measurements of neat ILs [19–23]. Recently, researchers have noticed that ILs have great potential for microwave absorption by studying the broadband dielectric properties of polymers based on ILs. For example, Tang *et al* measured the permittivities of four ILs in the solid state, i.e. P[VBBI][BF_4], P[VBBI][Sac], P[VBBI][$FeCl_4$], and P[VBTMA][BF_4], and found that these polymers had higher dielectric-loss factors (0.18–0.37) than other commonly used polymers [24]. More recently, our group realized a new structural microwave-absorbing material using [EMIm][$N(CN)_2$] ILs, and that a strong microwave-absorption rate of over 90% can be achieved over the entire frequency range 8.4–29.0 GHz. Thus, it is feasible to design ILs-based absorbing material [25], and, in order to design such material with better performance, it is necessary to systematically study both its dielectric and absorbing properties.

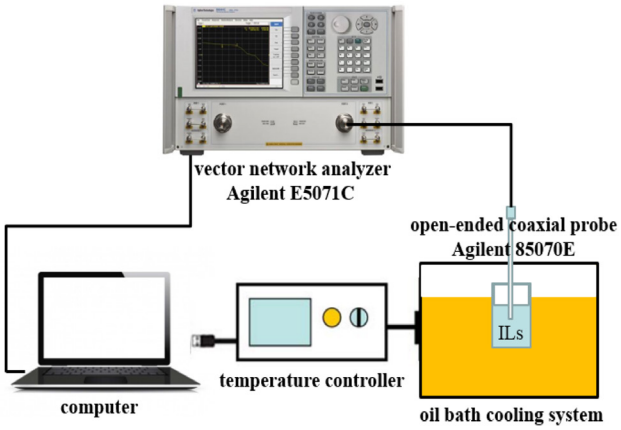

Figure 2. Complex permittivity measurement apparatus.

In the work reported in this paper, the dielectric properties of 12 [E and BMIm]$^+$-based ILs with different anions were measured by a typical open-ended coaxial probe system, and the measured results show that the ILs have high electromagnetic-loss properties, indicating a great potential application in microwave absorption. Furthermore, the absorption properties of ILs were studied systematically with the change of anions and cations in the range 1–14 GHz.

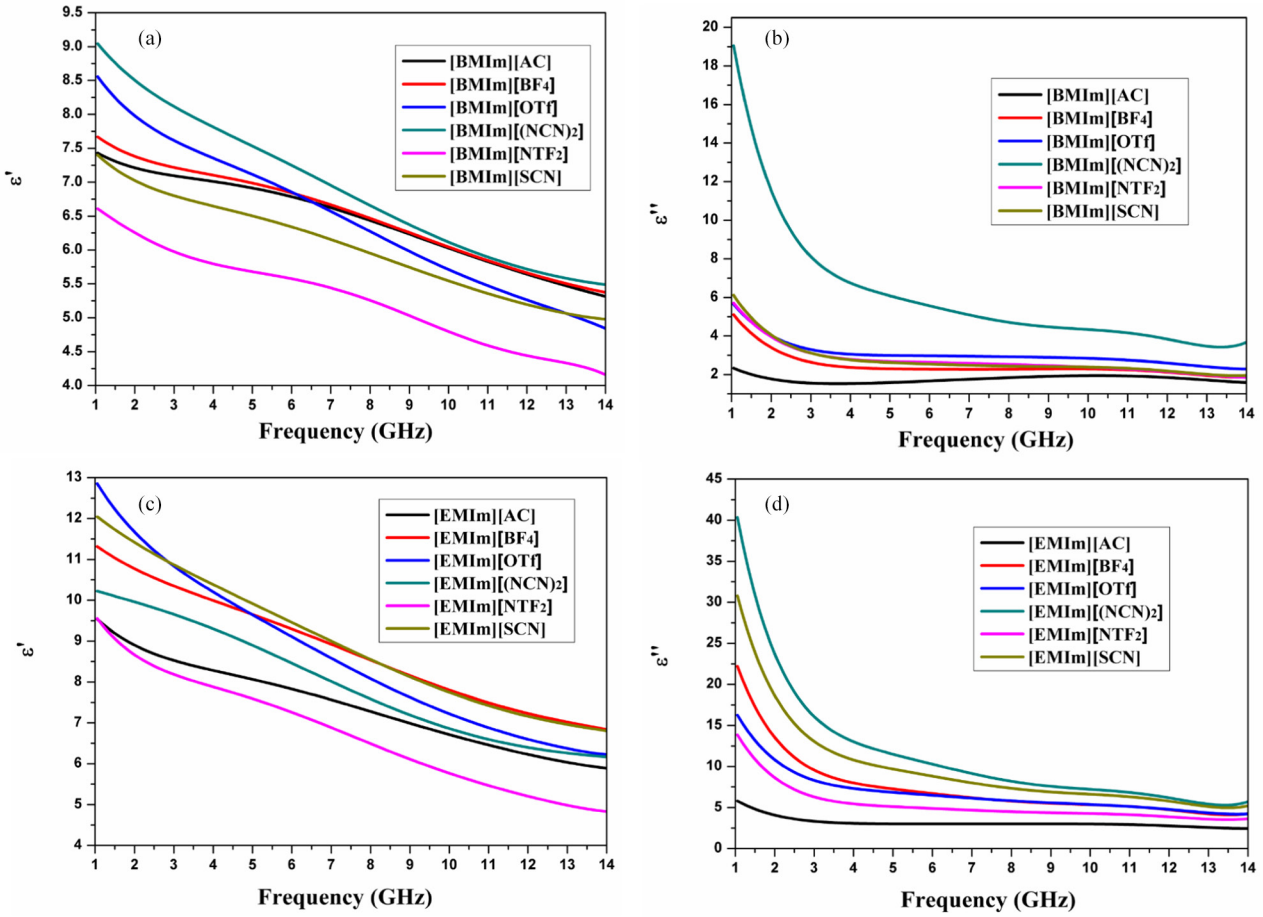

Figure 3. (a) Real and (b) imaginary parts for permittivity of $[BMIm]^+$-based; (c) real and (d) imaginary parts for permittivity of $[EMIm]^+$-based Ils.

In addition, the effect of temperature and coating thickness on absorbing properties was analyzed. It was found that ILs could be used as a novel class of liquid-absorbing materials that had the advantages of various types, flexible structure, and low cost.

2. Experimental section

2.1. Preparation of materials

Twelve [E and BMIm]$^+$-based RTILs, i.e. [BMIm][AC], [BMIm][BF_4], [BMIm][$N(CN)_2$], [BMIm][NTf_2], [BMIm][OTf], [BMIm][SCN], [EMIm][AC], [EMIm][BF_4], [EMIm][$N(CN)_2$], [EMIm][NTf_2], [EMIm][OTf], and [EMIm][SCN], were synthesized according to established procedures, and their structures were shown in figure 1. The purity of all the ILs was >99%. All ILs were carefully dried under vacuum at ~40 °C for at least 7 d, yielding water levels of <40 ppm as determined by Coulometric Karl Fischer titration.

2.2. Dielectric properties and DC conductivities measurement

The complex dielectric function can be expressed as $\varepsilon^*(\omega) = \varepsilon'(\omega) - i\varepsilon''(\omega)$, the real part of which, $\varepsilon'(\omega)$, reflects the dielectric dispersion, which signals how far the polarization of the sample is able to follow the oscillating electric field [26]. The imaginary part $\varepsilon''(\omega)$ reflects the dielectric loss cause by the absorption of electromagnetic radiation by the sample. It is difficult to measure the dielectric properties of conducting materials such like ILs, because the samples are largely short-circuited by high electrical conductance, conventional testing techniques can not detect them. Microwave-reflection spectroscopy can be a suitable tool to measure the dielectric constant ($\varepsilon'(\omega)$) and loss factor ($\varepsilon''(\omega)$) of highly conducting liquid samples. The dielectric properties of a series of ILs were measured using an open-ended coaxial probe system shown in figure 2 [18, 26].

The conductivities (σ) were measured by conductivity meter S230 Seven Compact™ with a precision of ±0.5%. Before measurements, the ILs were kept in oil bath to obtain a constant temperature.

3. Results and discussion

3.1. Dielectric properties

The dielectric properties of $[BMIm]^+$-based ILs are shown in figures 3(a) and (b). For the real part ($\varepsilon'(\omega)$), the values decrease from 9 to 4 with the increase of frequency (1–14

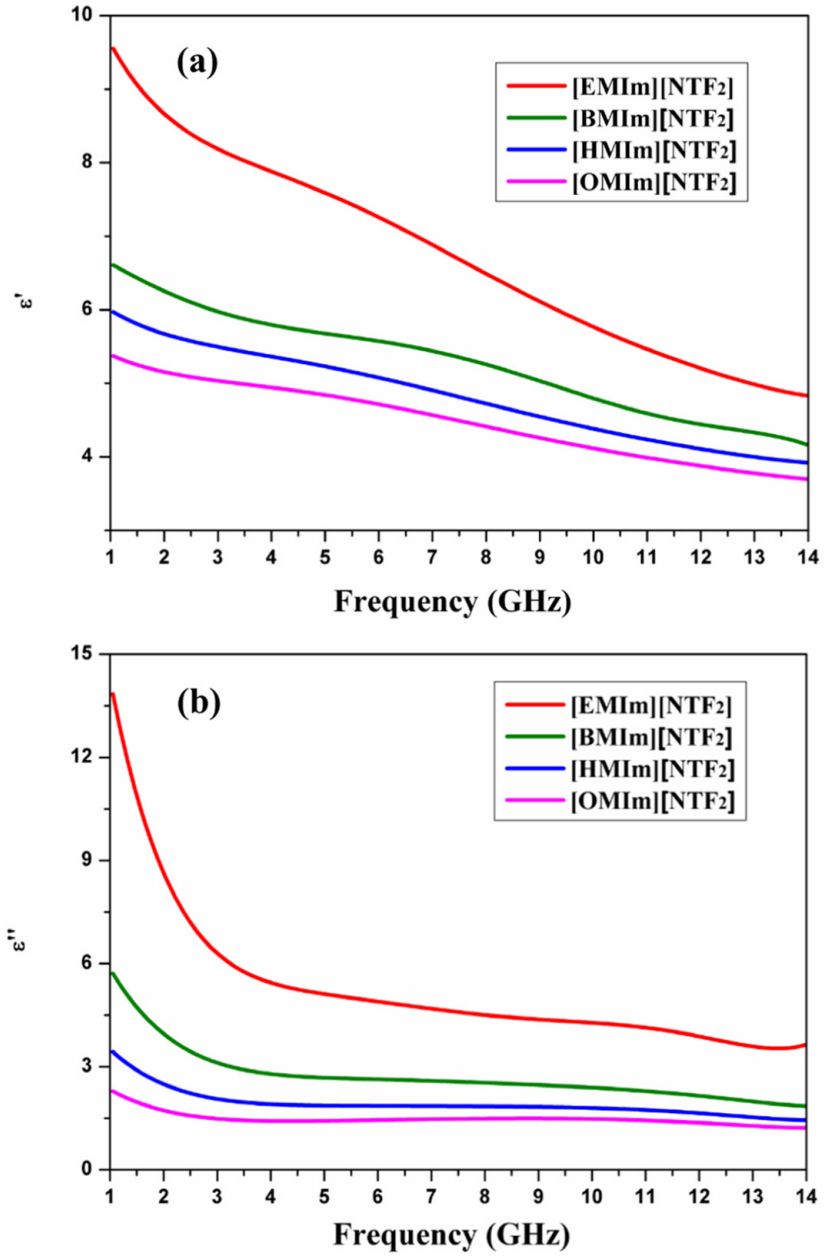

Figure 4. (a) Real parts and (b) imaginary parts for permittivity of $[NTF_2]^-$ -based ILs.

GHz). For the image part ($\varepsilon''(\omega)$), the values decline distinctly from 18.5 to 2 as the frequency increase from 1 to 4 GHz, and the values reduce gently as the frequency is higher than 4 GHz. For anions with symmetric structure, such as $[BF_4]^-$ and $[NTf_2]^-$, which lack a permanent dipole moment, the contribution to $\varepsilon'(\omega)$ mainly comes from the cation, and the values from these ILs are similar. With the increasing polarity of anions, the value $\varepsilon'(\omega)$ of ILs increases, which is attributed to the relaxation effect of the composites. Furthermore, the value $\varepsilon''(\omega)$ depends on conductance and polarization [27]. The dielectric properties of $[EMIm]^+$-based ILs are shown in figures 4(c) and (d). Compared to $[BMIm]^+$-based ILs, it is found that the dielectric properties change regularly in different frequency bands, which may be due to the change in anion and cation dipole-moment orientation [28]. In addition, the value becomes higher as the length of the alkyl chain decreases due to the effective dipole moment of cations decreasing from 7.0D to 2.5D [29]. In order to further confirm the influence of chain length, the dielectric properties of [HMIm][NTF_2] and [OMIm][NTF_2] with longer chain lengths were tested, and the results showed similar trend in figure 4. The dielectric properties of composites can be explained by the Debye theory. The Cole–Davidson model (formulas (1) and (2) below) has been validated for fitting the permittivity dispersion spectra [30], which means that ILs comprise an asymmetric Lorentzian medium. The $\varepsilon'(\omega)$ and $\varepsilon''(\omega)$ values of permittivity are expressed as

$$\varepsilon'(\omega) = \varepsilon_\infty + (\varepsilon_{st} - \varepsilon_\infty)\cos^\beta\varphi\cos(\varphi\beta), \quad (1)$$

$$\varepsilon''(\omega) = (\varepsilon_{st} - \varepsilon_\infty)\cos^\beta\varphi\sin(\varphi\beta) + \sigma/\omega\varepsilon_0, \quad (2)$$

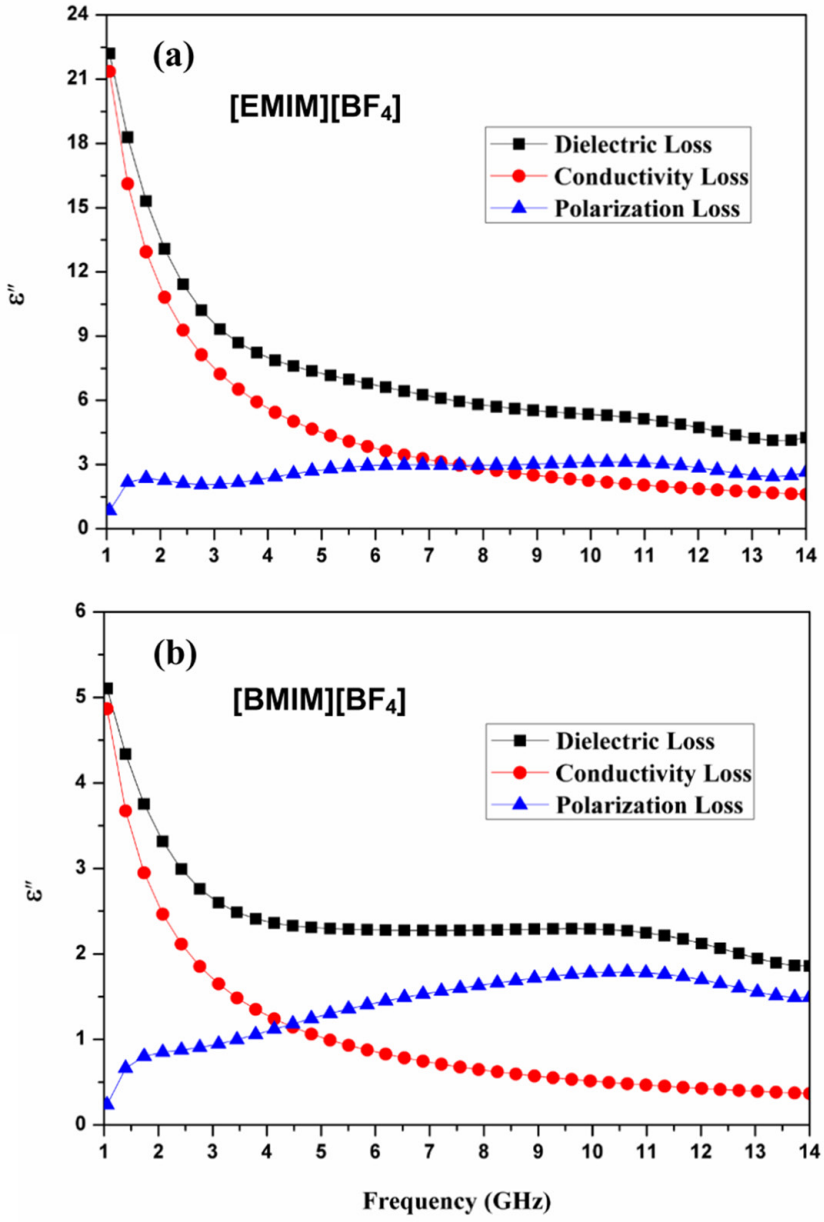

Figure 5. Experimental and fitting data of imagery permittivity of [EMIm][BF_4] (a) and [BMIm][BF_4] (b).

where $\varphi = \arctan \omega\tau$, ε_∞ is the permittivity when the frequency is infinity, ε_{st} is the static permittivity, ε_0 is the permittivity of free space, ω is the angular frequency, τ is the most probable relaxation time, σ is the DC conductivity, and β is an empirical constant with values between 0 and 1 that measures the distribution of relaxation times.

In the microwave-frequency range, the possible contributions to the complex dielectric function originate from different processes: Maxwell–Wagner polarization, rotational contributions, and translational contributions. As ILs are charged systems, the contribution from rotation and translation cannot be separated experimentally. To show the contribution of the conductivity loss and polarization loss to the $\varepsilon''(\omega)$ value clearly, we compared the experimental data of $\varepsilon''(\omega)$ and the conductivity loss (fitted by equation (2)) as shown in figure 5. Besides, the values of conductivity (σ) for [EMIm][BF_4] and [BMIm][BF_4] are 1.25 and 0.285 S m^{-1}, respectively. The results show that the conductivity loss decreases and the polarization loss first increases and then decreases with increasing frequency. In particular, the conductivity loss is found to be dominant for the dielectric loss in the low-frequency band, and the polarization loss plays a major role in high-frequency bands.

3.2. Microwave-absorption properties

Based on the measured data of the complex permittivity, and assuming that a single layer of ILs is attached on a metal plate, the electromagnetic-wave-absorbing properties could usually be evaluated by the following equations [31]:

$$\mathrm{RL} = 20 \log |(Z_{in} - Z_O)/(Z_{in} + Z_O)|, \qquad (3)$$

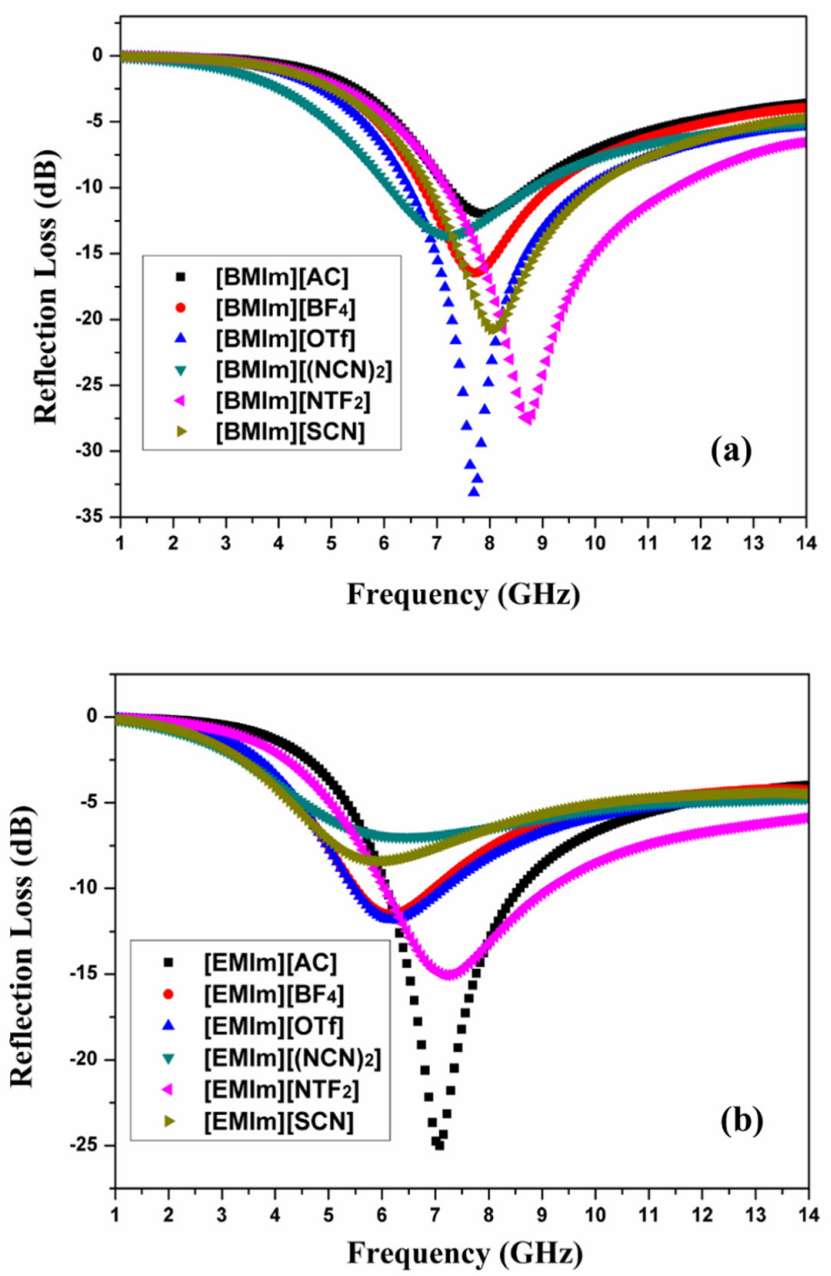

Figure 6. Microwave-absorbing properties of $[BMIm]^+$ (a)- and $[EMIm]^+$ (b) -based ILs.

$$Z_{in} = Z_0\sqrt{(\mu/\varepsilon\ )}\tanh[j(2\pi ft/c\ )\sqrt{\mu\varepsilon}], \quad (4)$$

where RL is the reflection loss, z_0 and z_{in} are the impedance of free space and the input characteristic impedance at the absorber/air interface, ε and μ are the measured relative complex permeability and permittivity, t and c represent thickness (m) and the speed of light in vacuum (3×10^8 m s^{-1}). The μ value of ILs is taken as 1 because of the weak magnetic property of the studied materials.

Figure 6(a) shows Microwave-absorbing properties of the $[BMIm]^+$-based ILs with a thickness of 4 mm in the frequency range 1–14 GHz. It is determined that the absorbing bandwidth is mainly concentrated in the range 6–12 GHz, and that the type of anions has an obvious effect on absorbing performances. For [BMIm][OTf], which has a maximum reflection loss (RL_M) of −33.1 dB at 7.70 GHz. [BMIm][NTf_2] has a great absorption bandwidth, which can reach up to 4.3 GHz bandwidth below −10 dB, and has a RL_M of −27.6 dB at 8.73 GHz. Figure 6(b) shows the reflection-loss characteristic curve of $[EMIm]^+$-based ILs, with the absorbing bandwidth mainly concentrated in the range 5–10 GHz. Compared with $[BMIm]^+$-based ILs, the RL_M moves to a lower frequency, and the effect of cations on absorption performance is also distinct. For [EMIm][OTf] and [EMIm][NTf_2], the RL_M are −12.4 dB at 6.02 GHz and −15.6 dB at 7.05 GHz and the absorption bandwidths are 1.5 and 3.1 GHz, respectively.

The mechanisms of energy loss are mainly due to dielectric and magnetic properties, which depend on the imaginary

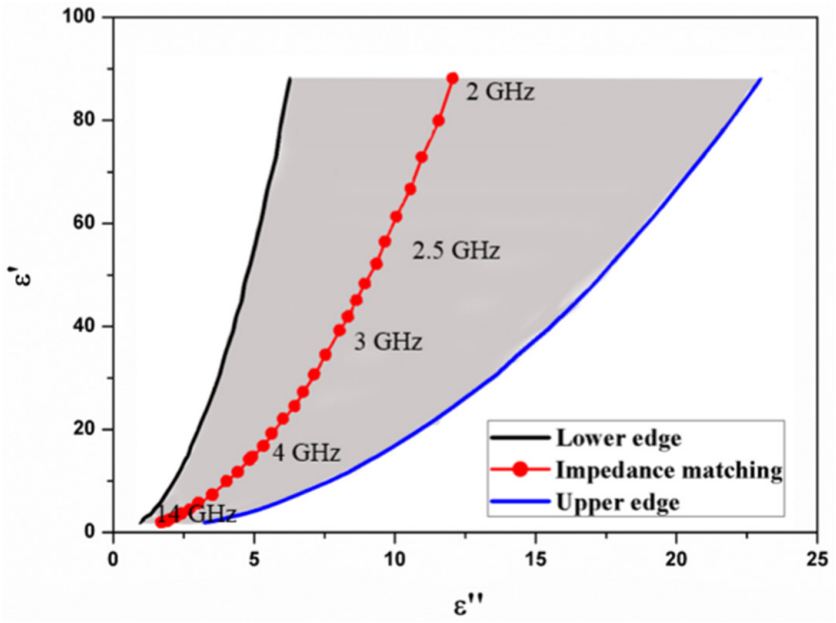

Figure 7. Permittivity distribution of the good microwave absorption (RL < -10 dB) and ideal absorption (RL < -60 dB) in the range 2 GHz (top)–14 GHz (bottom).

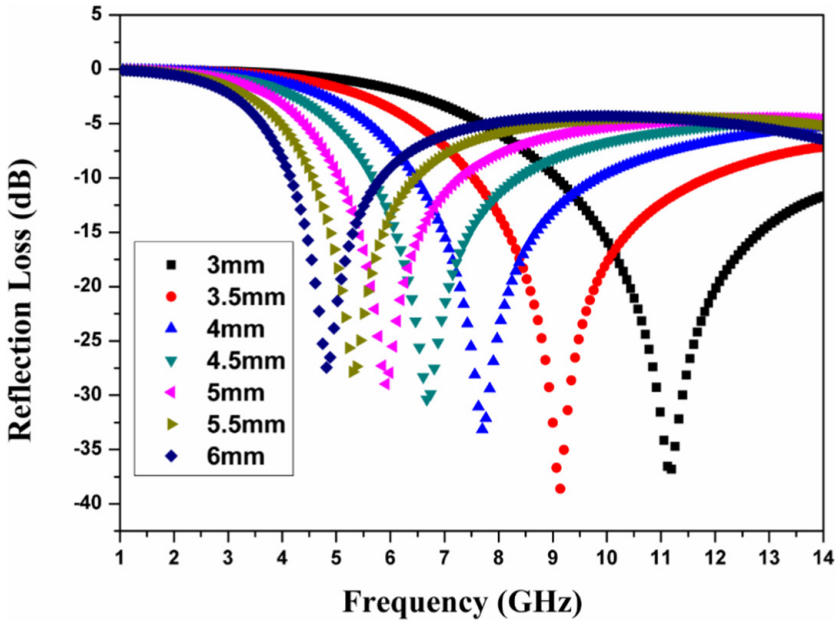

Figure 8. Reflection losses at different thicknesses.

part of the complex permittivity and complex permeability. Owing to the magnetism of ILs being weak, dielectric loss is the main microwave-absorbing mechanism of ILs. Another important concept related to microwave absorption is the impedance-matching characteristic. An overly large or overly small permittivity of the absorbing material is both harmful to the impedance matching and results in strong reflection and weak absorption. For clarity, the correlation between permeability and microwave absorbing properties was analyzed in the range 2–14 GHz based on equation (3), with the thickness of 4 mm, as shown in figure 7. It are found that if the materials show good microwave-absorbing performance (RL < -10 dB) and ideal absorption (RL < -60 dB), the permittivity must distribute in a specific area which between the upper and lower edges. Besides, the range of matching dielectric properties becomes smaller as the frequency increases. In the range 5–12 GHz, the matching values of $\varepsilon'(\omega)$ and $\varepsilon''(\omega)$ are from 14.4 to 2.8 and from 9.1 to3.8, respectively. Measurement results show that the and values of [E and BMIm]$^{+}$-based RTILs range from 10.2 to 4.5 and 12.1 to 2, respectively, which are mostly located in the permittivity distribution region with the good microwave absorption. Therefore, the difference of ideal matching dielectric properties (Ideal absorption) of various ILs would result in the distinction of the maximum reflection losses and peak frequency in figure 7. However, the quantitative relationship between complex permeability and

Table 1. Details of maximum reflection losses values of RL_M (dB) and peak frequency (FP) of $[BMIm]^+$-based ILs.

	[BMIm][AC]		[BMIm][BF_4]		[BMIm][$N(CN)_2$]		[BMIm][NTF_2]		[BMIm][SCN]		[BMIm][OTF]	
	FP	RL_M	FP	RL_M	FP	RL_M	FP	RL_M	FP	RL_M	FP	RL_M
3 mm	10.92	−14.02	10.85	−17.99	10.23	−15.40	12.56	−20.67	11.4	−20.60	11.19	−36.80
3.5 mm	9.21	−13.20	9	−17.34	8.45	−14.83	10.37	−26.70	9.48	−21.44	9.14	−38.61
4 mm	7.90	−11.99	7.70	−16.45	7.22	−13.63	8.73	−27.61	8.04	−20.73	7.70	−33.14
4.5 mm	6.88	−11.07	6.74	−16.02	6.26	−12.52	7.56	−27.77	7.01	−20.69	6.67	−30.37
5 mm	6.12	−10.41	5.99	−15.81	5.51	−11.76	6.67	−27.95	6.26	−20.95	5.92	−28.97
5.5 mm	5.57	−9.94	5.44	−15.73	4.96	−11.21	6.05	−28.20	5.64	−21.29	5.30	−27.84
6 mm	5.03	−9.60	4.96	−15.75	4.48	−10.75	5.51	−28.59	5.10	−21.74	4.82	−27.44

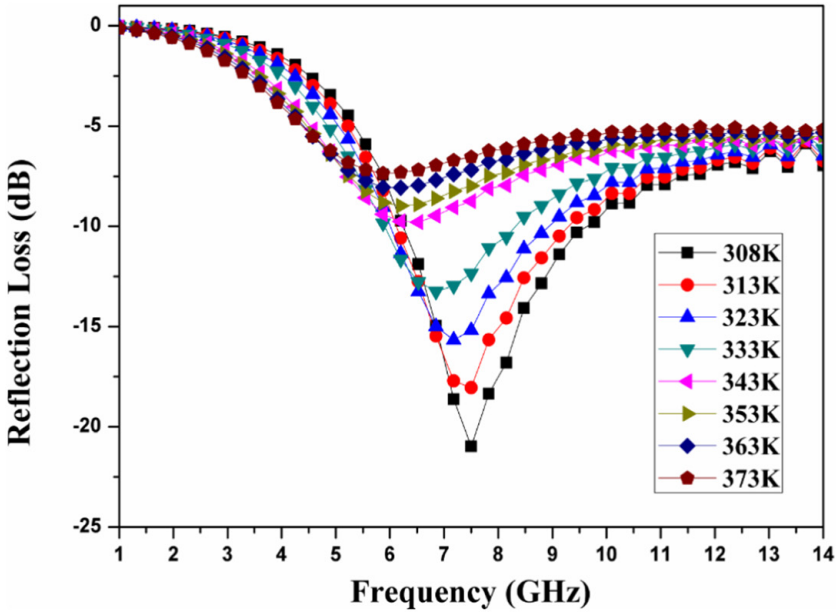

Figure 9. Reflection losses at different temperatures.

Table 2. Change in maximum reflection losses values of RL_M (dB) and peak frequency (FP) of $[BMIm]^+$-based ILs with different temperatures.

	[BMIm][AC]		[BMIm][BF_4]		[BMIm] [$N(CN)_2$]		[BMIm][NTF_2]		[BMIm][SCN]		[BMIm][OTF]	
	FP	RL_M	FP	RL_M	FP	RL_M	FP	RL_M	FP	RL_M	FP	RL_M
308 K	7.46	−48.31	7.44	−26.39	6.98	−8.85	7.9	−19.38	4.32	−11.99	7.50	−20.05
313 K	7.31	−33.90	7.31	−23.04	6.92	−8.71	7.68	−17.77	4.24	−10.86	7.31	−18.44
323 K	7.24	−25.51	7.11	−16.57	6.66	−7.22	7.37	−15.53	4.12	−9.13	7.24	−16
333 K	7.05	−18.58	6.79	−12.21	6.46	−6.24	7.15	−13.39	4.06	−7.35	7.05	−13.30
343 K	6.78	−16.15	6.61	−10.08	6.32	−5.36	7.03	−11.86	3.86	−6.01	6.33	−9.90
353 K	6.59	−13.87	6.48	−8.30	6.20	−5.04	6.92	−10.68	3.86	−4.97	6.14	−9.01
363 K	6.33	−11.76	6.33	−7.25	6.14	−4.49	6.73	−9.51	3.86	−4.97	5.94	−8.07
373 K	6.14	−10.22	6.20	−7.09	6.01	−4.03	6.40	−7.86	3.86	−4.97	5.88	−7.37

the maximum reflection losses seemed not clear at current stage, and we will study in-depth in the following work.

As previously stated, [BMIm][OTf] showed excellent absorption performance in the measured frequency ranges. To study the microwave-absorption performance in depth, the effect of coating thickness and temperature was studied in detail. Figure 8 shows the RL of the [BMIm][OTf]-based ILs with different thicknesses in the range 1–14 GHz. It is observed that the thickness of the absorbing material has a great influence on the microwave-absorbing properties. In addition, the RL_M gradually shifts toward a lower frequency with increasing thickness. When the thickness is 3 mm, the RL_M that can be achieved is −36.5 dB at 11.2 GHz, and the absorption bandwidth can reach up to 4.9 GHz (from 9.1 to 14 GHz). When the thickness is 3.5 mm, the RL_M increases to −38.6 dB at 9.14 GHz, and the absorption bandwidth

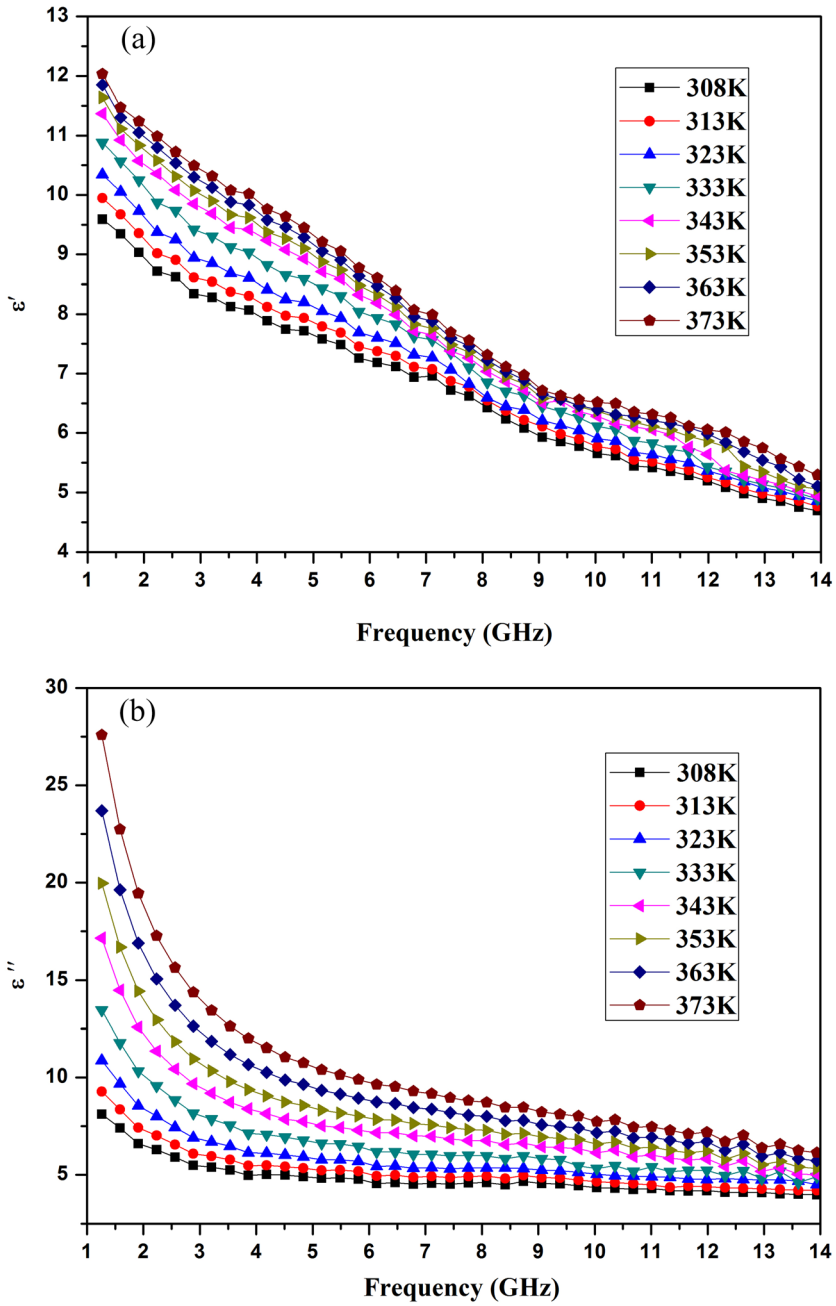

Figure 10. (a) Real parts and (b) imaginary parts for permittivity of [BMIm][OTf] versus frequency and temperature.

is 4.3 GHz (from 7.5 to 11.8 GHz). The RL_M gradually decreases and the absorption peak frequency (FP, denoting the frequency of RL_M) gradually shifts to lower frequencies with increasing coating thickness from 4 to 6 mm in steps of 0.5 mm. The detailed comparison of the RL_M and FP for the $[BMIm]^+$-based ILs values are shown in table 1. In the investigated region, the RL_M easily reach below −10 dB, and FP with effective absorption over the full C band (4–8 GHz) and X band (8–12 GHz) are observed.

Figure 9 plots the RL of [BMIm][OTf] versus different frequencies and temperatures at a thickness of 4 mm. It is found that the RL_M gradually decreases and the FP gradually shifts to lower frequencies with increasing temperature. It is implied that the microwave absorption of [BMIm][OTf] at lower temperature is greater than that at higher temperature. The $[BMIm]^+$-based ILs RL values depend on frequency and temperature change similarly as in table 2.

On the basis of the experimental data, we next discuss the variation of RL with changing temperature and thickness. According to the impedance-matching conditions of microwave absorption, to meet the requirement of attenuation A(dB), the electromagnetic parameters, thickness, and frequency should follow the constraint conditions [32]:

$$\varepsilon' = \frac{\pi c}{2t\omega}\coth\left(\frac{\pi}{2}\tan\delta\right)\frac{1-10^{-A/20}}{1+10^{-A/20}}, \tag{5}$$

$$\varepsilon'' = \varepsilon' \times \tan\delta \tag{6}$$

where c is the speed of light in vacuum, t is the thickness, and ω is the angular frequency. From equations (5) and (6) we can find that the dielectric-loss factor $\tan\delta$, frequency, and thickness have effects on A(dB). Accordingly, when the electromagnetic wave is transmitting in the medium, the peak frequency f can be expressed as [33]

$$f = \frac{c}{4t[Real(\sqrt{\varepsilon\mu})]}. \quad (7)$$

The $\varepsilon'(\omega)$ and $\varepsilon''(\omega)$ values of [BMIm][OTf] clearly increases with increasing temperature, as shown in figure 10, and the $\varepsilon'(\omega)$ and $\varepsilon''(\omega)$ values of other ILs exhibit a similar trend, which makes the impedance between air and ILs deviate from the initial impedance-matching condition. As a consequence, this deviation leads to the variation of RL.

4. Conclusions

In this paper, the dielectric and absorbing properties of [E and BMIm]$^+$-based RTILs were investigated in the 1–14 GHz microwave-frequency range. The $\varepsilon'(\omega)$ values decrease from 13 to 4 and the $\varepsilon''(\omega)$ values decrease from 40 to 1.5, which are mostly located in the permittivity distribution region with the good microwave absorption. The dielectric properties become higher as the length of the alkyl chain decreases due to the effective dipole moment of cations decreasing from 7.0D to 2.5D. With increasing anion polarity, the $\varepsilon'(\omega)$ values of the ILs increase, which is attributed to the relaxation effect of the composites. The $\varepsilon''(\omega)$ values depend on conductance and polarization. Furthermore, the conductivity loss is found to be dominant for dielectric loss in the low-frequency band, and the polarization loss plays a major role in high-frequency bands. The [E and BMIm]$^+$-based RTILs have good absorption properties, and the absorption bands are mainly concentrated in the C bands (4–8 GHz) and X bands (8–12 GHz). Moreover, the microwave absorption can be tuned easily by varying the anions and cations. The absorption peak frequency of the ILs gradually moves to low frequency with increasing temperature and coating thickness. It is believed that ILs could be used as a novel class of liquid-state material composites that will find wide application in the microwave-absorbing area.

Acknowledgments

This work was supported by the National Key Research and Development Program of China (2017YFA0403101) and the Fundamental Research Funds for the Central Universities (lzujbky-2015-315, lzujbky-2016-141). Natural Science Foundation of Gansu Province (17JR5RA119).

ORCID iDs

Fulong Yang https://orcid.org/0000-0003-3307-1190
Xiaoping Zhang https://orcid.org/0000-0003-0046-211X
Youquan Deng https://orcid.org/0000-0002-7612-0354

References

[1] Wen B *et al* 2014 *Adv. Mater.* **26** 3484–9
[2] Kong L, Yin X W, Yuan X Y, Zhang Y J, Liu X M, Cheng L F and Zhang L T 2014 *Carbon* **73** 185–93
[3] Zhang Y, Huang Y, Zhang T F, Chang H C, Xiao P S, Chen H H, Huang Z Y and Chen Y S 2015 *Adv. Mater.* **27** 2049–53
[4] Sun H, Che R C, You X, Jiang Y S, Yang Z B, Deng J, Qiu L B and Peng H S 2014 *Adv. Mater.* **26** 8120–5
[5] Qing Y C, Wen Q L, Luo F and Zhou W C J 2016 *J. Mater. Chem.* C **4** 4825–6
[6] Qing Y C, Wen Q L, Luo F, Zhou W C and Zhu D M J 2016 *J. Mater. Chem.* C **4** 371–5
[7] Yousefi N, Sun X Y, Lin X Y, Shen X, Jia J J, Zhang B, Tang B Z, Chan M S and Kim J K 2014 *Adv. Mater.* **26** 5480–7
[8] Ling K Y, Yoo M Y, Su W J, Kim K, Cook B, Tentzeris M M and Lim S 2015 *Opt. Express* **23** 110–20
[9] Stankovich S, Dikin D A, Dommett G H B, Kohlhaas K M, Zimney E J, Stach E A, Piner R D, Nguyen S T and Ruoff R S 2006 *Nature* **442** 282–6
[10] Qing Y C, Nan H Y, Luo F and Zhou W C 2017 *RSC Adv.* **7** 27755–61
[11] Yoo Y J, Ju S H, Park S Y, Kim Y J, Bong J H, Lim T Y, Kim K W, Rhee J Y and Lee Y P 2015 *Sci. Rep.* **5** 14018
[12] Zhu W M *et al* 2015 *Adv. Mater.* **27** 4739–43
[13] Plechkova N V and Seddon K R 2008 *Chem. Soc. Rev.* **37** 123–50
[14] Shiddiky M J and Torriero A A 2011 *Biosens. Bioelectron.* **26** 1775–87
[15] Agudelo Mesa L B, Padro J M and Reta M 2013 *Food Chem.* **141** 1694–701
[16] Wakai C, Oleinikova A, Ott M and Weingärtner H 2005 *J. Phys. Chem.* B **109** 17028–30
[17] Weingärtner H 2006 *Z. Phys. Chem.* **220** 1395–405
[18] Huang M M, Jiang Y P, Sasisanker P, Driver G W and Weingärtner H 2011 *J. Chem. Eng. Data* **56** 1494–9
[19] Sangoro J R, Mierzwa M, Iacob C, Paluch M and Kremer F 2012 *RSC Adv.* **2** 5047–50
[20] Hensel-Bielowka S *et al* 2015 *J. Phys. Chem.* C **119** 20363–8
[21] Sippel P, Lunkenheimer P, Krohns S, Thoms E and Loidl A 2015 *Sci. Rep.* **5** 13922
[22] Yamada S A, Bailey H E, Tamimi A, Li C Y and Fayer M D 2017 *J. Am. Chem. Soc.* **139** 2408–20
[23] Huang M M and Weingärtner H 2008 *Chem. Phys. Chem.* **9** 2172–3
[24] Tang J B, Radosz M and Shen Y Q 2008 *Macromolecules* **41** 493–6
[25] Gong J H, Yang F L, Shao Q F, He X D, Zhang X P, Liu S M, Tang L Y and Deng Y Q 2017 *RSC Adv.* **7** 41980–8
[26] Weingärtner H 2014 *J. Mol. Liq.* **192** 185–91
[27] Alexander S, Hunger J, Buchner R, Hefter G, Thoman A and Helm H 2008 *J. Phys. Chem.* B **112** 4854–8
[28] Jin H, O'Hare B, Dong J, Arzhantsev S, Baker G A, Wishart J F, Benesi A J and Maroncelli M 2008 *J. Phys. Chem.* B **112** 81–92
[29] Hunger J, Stoppa A, Buchner R and Hefter G 2009 *J. Phys. Chem.* **113** 9527–37
[30] Zhou W C, Hu X J, Bai X X, Zhou S Y, Sun C H, Yan J and Chen P 2011 *ACS Appl. Mater. Interfaces* **3** 3839–45
[31] Hunger J, Stoppa A, Schrödle S, Hefter G and Buchner R 2009 *ChemPhysChem* **10** 723–33
[32] Huynen I, Quiévy N, Bailly C, Bollen P, Detrembleur C, Eggermont S, Molenberg I, Thomassin J M, Urbanczyk L and Pardoen T 2011 *Acta Mater.* **59** 3255–66
[33] Wang B C, Wei J Q, Yang Y, Wang T and Li F 2011 *J. Magn. Mater.* **323** 1101–3